Supplementary Materials

Preparation of boronate affinity-functionalized metal-organic framework material for selective recognition and separation of glycoprotein under physiological pH

Baoyue Zhang[a,#], Xue Chen[a,#], Jianghua He[b], Bailin Guo[a], Sheng Bi[a], Feng Zhang[a,*],

Miaomiao Tian[a,*]

[a] *College of Chemistry and Chemical Engineering, Harbin Normal University, Harbin 150025, P. R. China.*

[b] *Ruyuan Hec Pharm Co., Ltd. Guangdong Province, Shaoguan 512700, P. R. China.*

[#] These authors contributed equally in this work.

1. Experimental

1.1 Equilibrium and adsorption kinetics experiments

     The adsorption equilibrium and adsorption kinetics of the material were studied by batch mode experiments. In the study of adsorption kinetics, 5 mg Zr-MOF@S-S@B adsorbent was added into a centrifuge tube with a concentration of 1 mg mL^{-1} OVA solution (5 mL, pH 8.5) to investigate the adsorption effect of different oscillation time. In isothermal adsorption test, 5 mg of Zr-MOF@S-S@B adsorbent was added to different concentrations of 5 mL OVA solution (pH 8.5). The adsorbents were separated from the solution, and the supernatant was passed through 0.45 μm filter membranes and detected by a UV-vis spectrophotometer.

[*] Corresponding authors. *E-mail*: Zhangfeng@hrbnu.edu.cn (F. Zhang); mmttqqq@163.com (M.M. Tian).

25   The adsorption kinetic models were evaluated by the pseudo-first-order kinetic model

26 and the pseudo-second-order kinetic model, which are calculated according to Eqn. (1) and

27 Eqn. (2), respectively.

28 $$\ln(Q - Q_t) = \ln Q - K_1 t \qquad (1)$$

29 $$\frac{t}{Q_t} = \frac{1}{K_2 Q^2} + \frac{t}{Q} \qquad (2)$$

30 where Q_t (mg g^{-1}) is the adsorption amount of OVA at time t (min). K_1 (L min^{-1}) and K_2 (mg

31 g^{-1} min^{-1}) are the rate constants of the pseudo-first-order kinetic model and the pseudo-

32 second-order kinetic model, respectively. The initial adsorption rate h (mg g^{-1} min^{-1}) and the

33 half-equilibrium time $t_{1/2}$ (min) can be calculated from the Eqn. (3) and Eqn. (4).

34 $$h = K_2 Q^2 \qquad (3)$$

35 $$t_{1/2} = \frac{1}{K_2 Q} \qquad (4)$$

36   The results of isothermal adsorption were evaluated by the Langmuir isothermal model

37 and the Freundlich isothermal model. Langmuir and Freundlich adsorption isotherms are

38 presented in Eqn. (5) and Eqn. (6), respectively.

39 $$\frac{1}{Q} = \frac{1}{Q_m} + \frac{1}{K_L Q_m C_e} \qquad (5)$$

40 $$\lg Q = \lg K_F + \frac{1}{n} \lg C_e \qquad (6)$$

41 where C_e (mg mL^{-1}) is the equilibrium concentration of OVA (mg mL^{-1}) in the solution, Q

42 (mg g^{-1}) is the amount of OVA adsorbed at the equilibrium. Q_m (mg g^{-1}) is the maximum

43 adsorption capacity of the adsorbent, K_L (mL mg^{-1}) is the Langmuir constant, K_F (mg g^{-1}) is

44 the Freundlich constant, and 1/n is the dimensionless constant.

45

46 **2. Results and discussion**

47

48 *2.1 Adsorption equilibrium and kinetics experiments*

49

50   There is an important relationship between adsorption kinetics and adsorption efficiency.

51 As shown in Fig. S3, Zr-MOF@S-S@B and reach equilibrium at 80 min. Fig. S4 (A) and

52 S4(B) are the curves of the pseudo-first-order dynamics model and the pseudo-second-order

53 dynamics model, which are calculated according to Eqs. (1) and (2). Table S1 describes the

54 relevant data fitting. Q_{exp} represents the maximum adsorption of the OVA measured in the

55 experiment, and Q_{tf} and Q_{ts} represent the equilibrium adsorption of the OVA in the pseudo-

56 first-order and pseudo-second-order kinetic equations, respectively. It can be seen from Table

57 S2 that the linear correlation coefficient (R^2) of pseudo-second-order dynamics is greater than

58 that of pseudo-first-order dynamics. It shows that the material is more consistent with the

59 pseudo-second-order dynamics model. It is suggested that the adsorption process is mainly

60 controlled by the chemical interaction between adsorbents and OVA.

61   The adsorption amount obtained by adsorption equilibrium is of great significance for

62 the optimization of adsorbents. As shown in Fig. S4 (C) and (D), Langmuir adsorption

63 isotherm model and Freundlich adsorption isotherm model were used to evaluate the

64 adsorption capacity. Table S3 shows the relevant fitting data calculated according to Eqs. (3)

65 and (4). The Langmuir linear correlation coefficient is (R^2 = 0.9716, 0.9422) and the

66 Freundlich linear correlation coefficient is (R^2 = 0.4125, 0.4020), indicating that the

67 adsorption   conforms   to   the   Langmuir   adsorption   model.

68 **Captions**

69 **Fig. S1** Zeta potential of Zr-MOF, Zr-MOF@SH, and Zr-MOF@S-S@B.

70 **Fig. S2** Optimization of synthesis conditions (A) MPTES content, (B) MPBA content.

71 **Fig. S3** Effect of adsorption time on adsorption capacity.

72 **Fig. S4** (A) Pseudo-first-order kinetic model, (B) pseudo-second-order kinetic model, (C)

73 Langmuir model, (D) Freundlich model.

74 **Fig. S5** Selective adsorption capacities of Zr-MOF, Zr-MOF@SH, and Zr-MOF@S-S@B

75 towards OVA, HRP, BSA, and Lyz.

76 **Fig. S6** Reusability of Zr-MOF@S-S@B.

77 **Fig. S7** CD images of OVA and OVA eluent.

78 **Fig. S8** UV spectra of protein powder solution (1.0 mg mL^{-1}), protein powder solution

79 pretreated by Zr-MOF@S-S@B, eluted by DTT.

80 **Table S1** Element content of Zr-MOF@S-S@B.

81 **Table S2** Pseudo-first-order and pseudo-second-order adsorption kinetics model data

82 parameters.

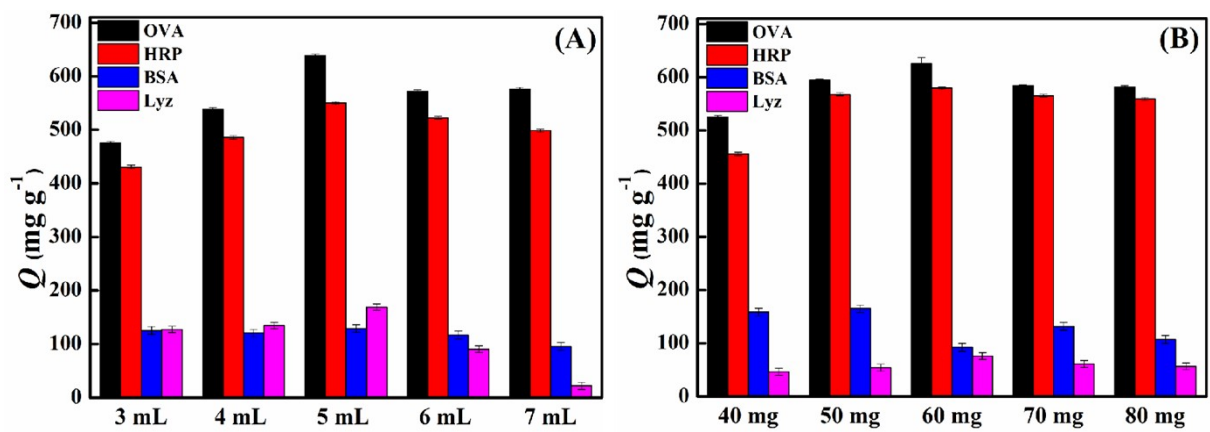83 **Table S3** The data parameters of Langmuir model and Freundlich model.
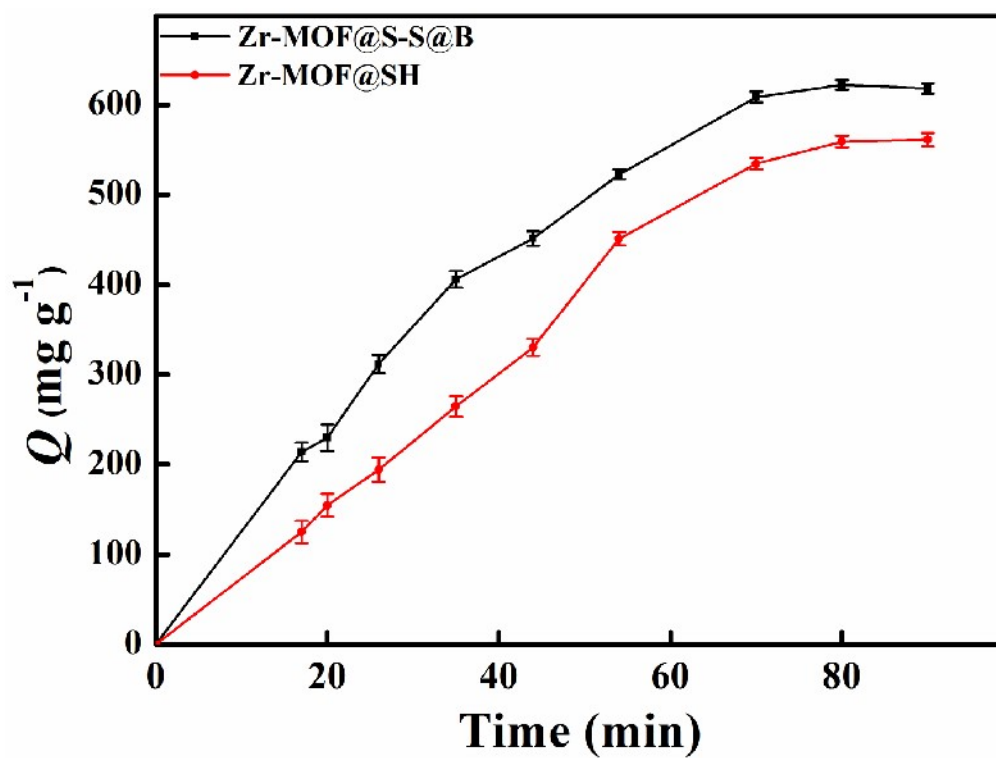
84

85
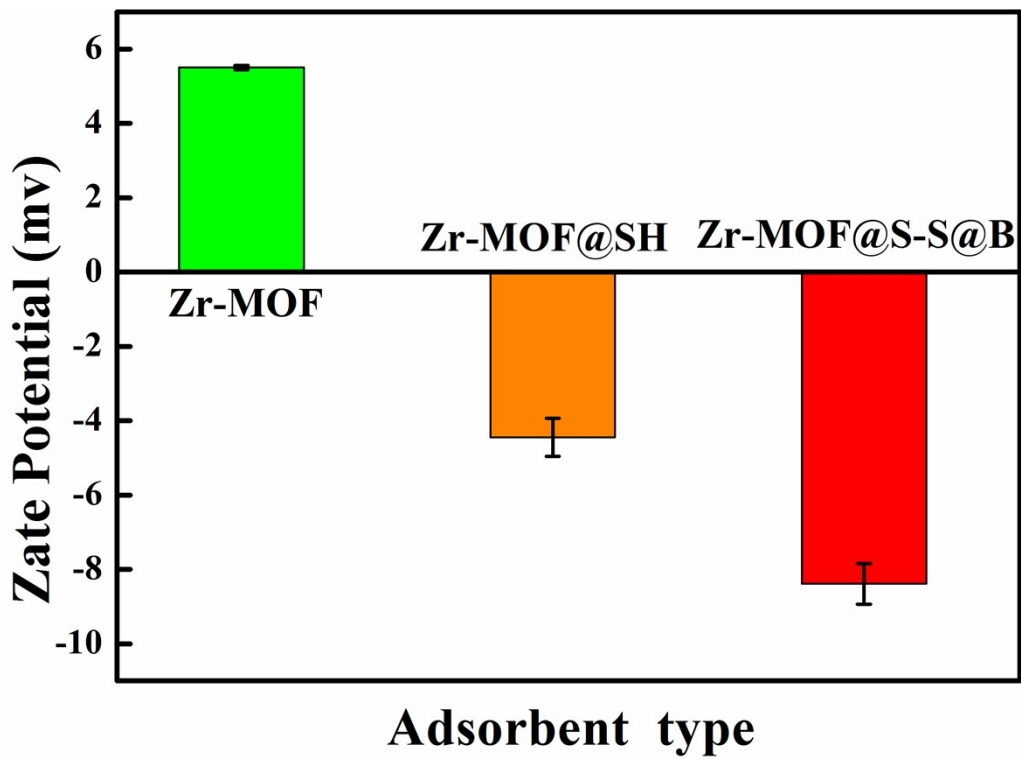
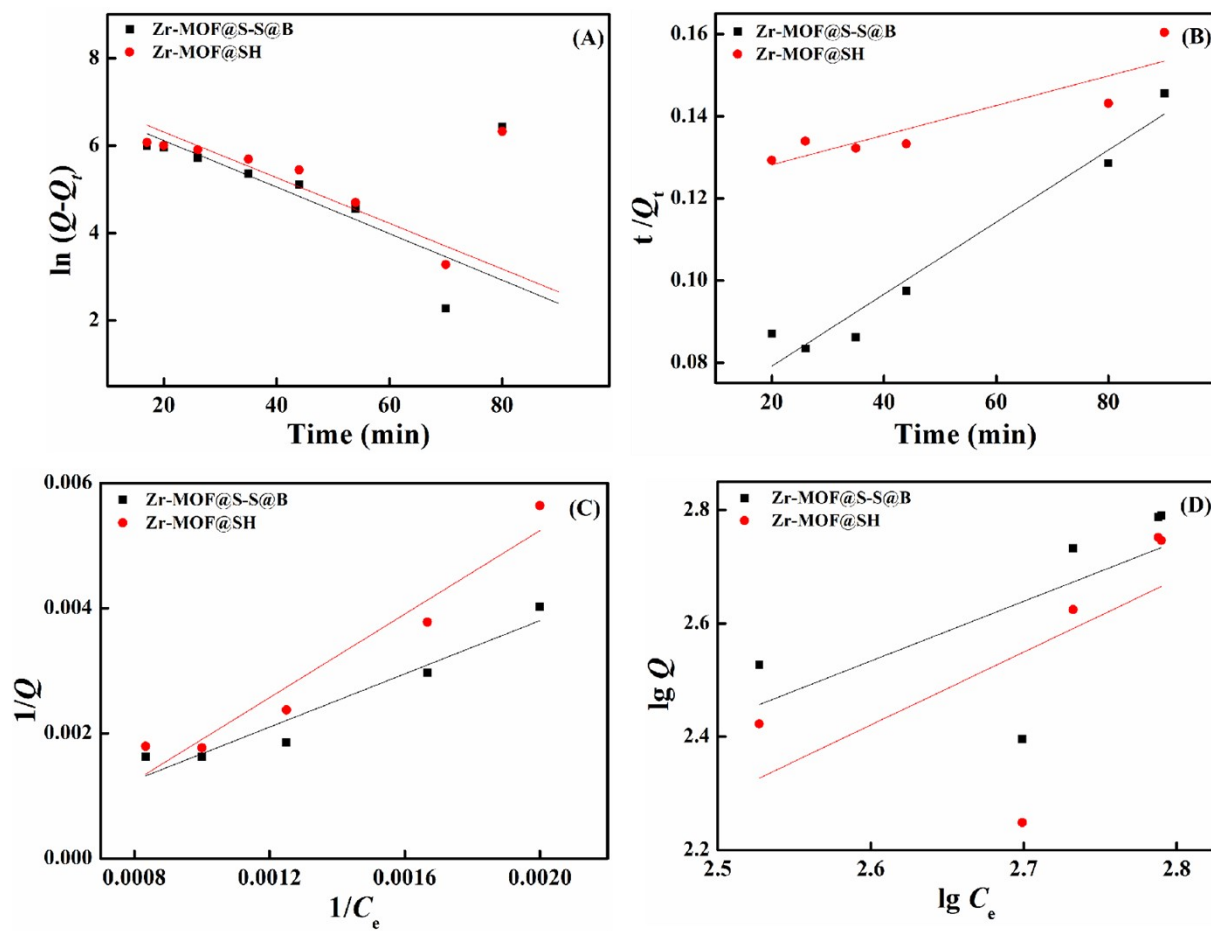**Fig. S1** Zeta potential of Zr-MOF, Zr-MOF@SH, and Zr-MOF@S-S@B.

87

88

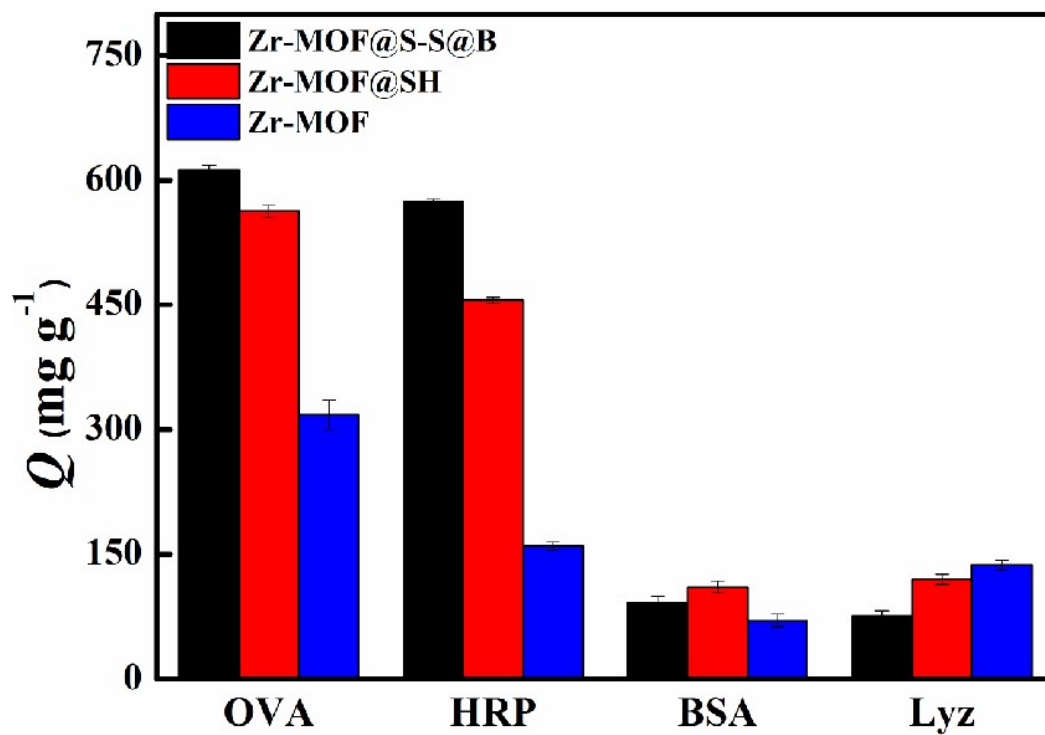**Fig. S2** Optimization of synthesis conditions (A) MPTES content, (B) MPBA content.

90

91 **Fig. S3** Effect of adsorption time on adsorption capacity.

92

93

Fig. S4 (A) Pseudo-first-order kinetic model, (B) pseudo-second-order kinetic model, (C) Langmuir model, (D) Freundlich model.
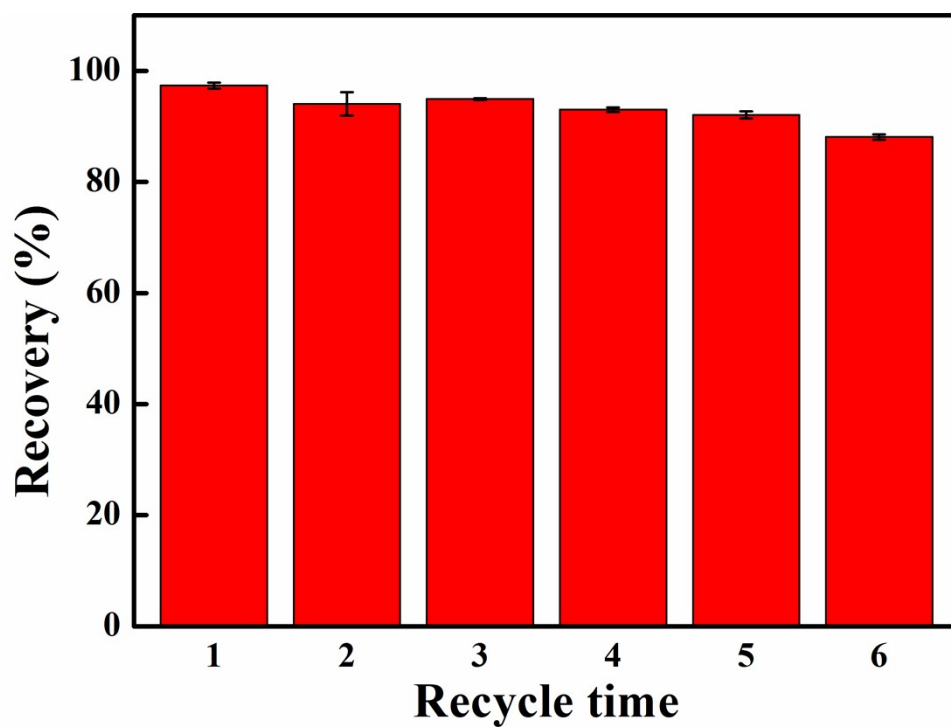
96

97

Fig. S5 Selective adsorption capacities of Zr-MOF, Zr-MOF@SH, and Zr-MOF@S-S@B
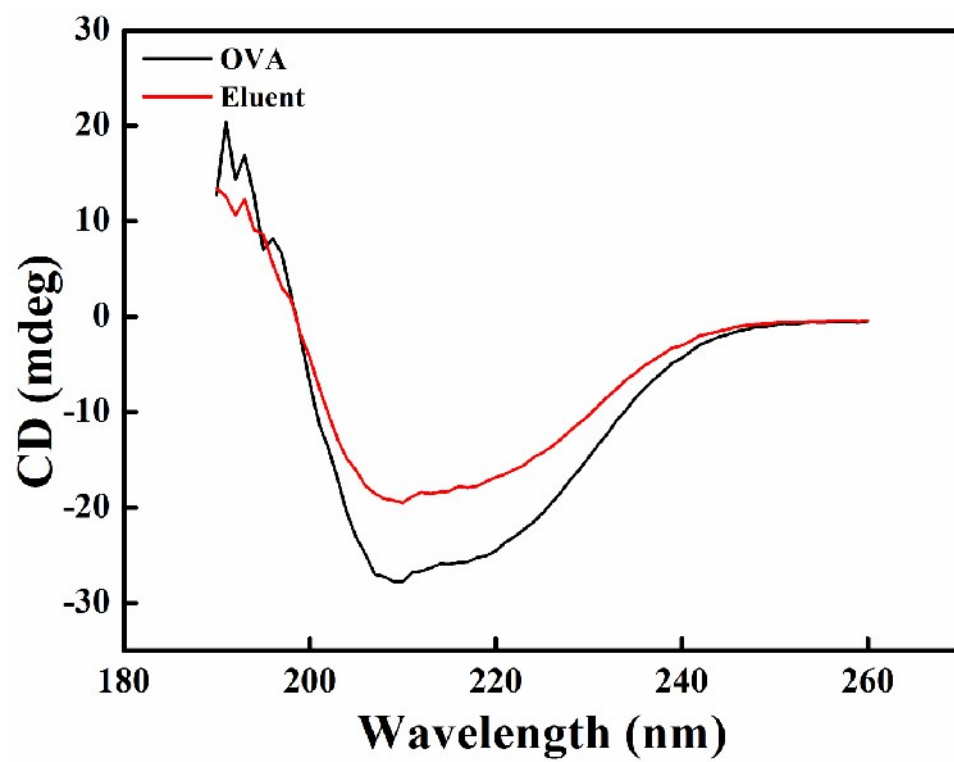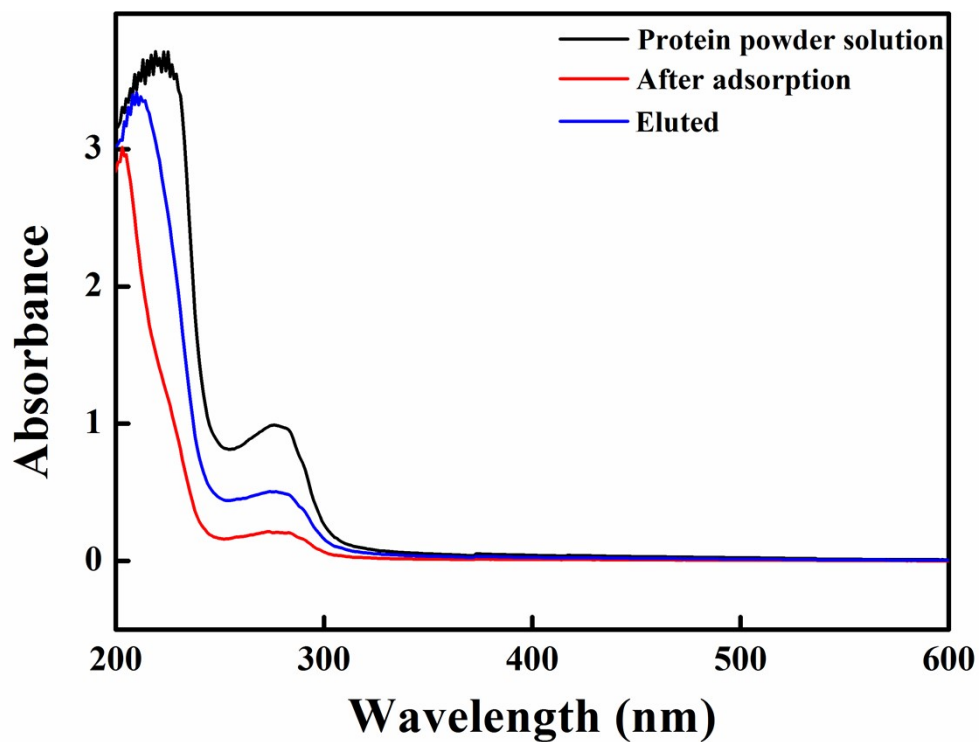
towards OVA, HRP, BSA, and Lyz.

100

101

102

Fig. S6 Reusability of Zr-MOF@S-S@B.

104

105

106 **Fig. S7** CD images of OVA and OVA eluent.

107

108

109

110 **Fig. S8** UV spectra of protein powder solution (1.0 mg mL-1), protein powder solution

111 pretreated by Zr-MOF@S-S@B, eluted by DTT.

112

113

114 **Table S1** Element content of Zr-MOF@S-S@B.

Element	Element weight (%)
C1s	57.04
B1s	23.24
O1s	18.31
S2p	0.41

Table S2 Pseudo-first-order and pseudo-second-order adsorption kinetics model data parameters.

Adsorbents	Q_{exp} (mg g^{-1})	Pseudo-first-order kinetic model			Pseudo-second-order kinetic model			h (mg g^{-1} min^{-1})	$t_{1/2}$ (min)
		Q_{tf} (mg g^{-1})	k_1 (min^{-1})	R^2	Q_{ts} (mg g^{-1})	k_2 (g mg^{-1} min^{-1})	R^2		
Zr-MOF@S-S@B	625.5	1295.6	0.0532	0.4521	598.8	0.0035	0.9579	16.23	67.93
Zr-MOF@SH	558.9	1496.6	0.0522	0.4695	522.9	0.0076	0.8187	82.63	30.26

Table S3 The data parameters of Langmuir model and Freundlich model.

Adsorbents	Langmuir model			Freundlich model		
	Q_m (mg g^{-1})	K_L (mL mg^{-1})	R^2	K_F (mg g^{-1})	$1/n$	R^2
Zr-MOF@S-S@B	1000	4.068×10^{-4}	0.9716	0.6210	1.054	0.4125
	714.2	4.194×10^{-4}	0.9422	0.1192	1.286	0.4020